Simultaneous reduction in cloud point, smoke, and NO_x emissions by blending bioethanol into biodiesel fuels and exhaust gas recirculation

T Shudo[1]*, **T Nakajima**[2], and **K Hiraga**[2]
[1]Division of Energy and Environmental Systems, Hokkaido University, Sapporo, Japan
[2]Toyota Motor Corporation, Aichi, Japan

The manuscript was accepted after revision for publication on 11 July 2008.

DOI: 10.1243/14680874JER01908

Abstract: Palm oil has the important advantage of productivity compared with other vegetable oils such as rapeseed oil and soybean oil. However, the cold flow performance of palm oil methyl ester (PME) is poorer than other vegetable-oil-based biodiesel fuels. Previous research by the current authors has shown that ethanol blending into PME improves the cold flow performance and considerably reduces smoke emission. The reduced smoke may be expected to allow an expansion in the exhaust gas recirculation (EGR) limit and lead to reduced oxides of nitrogen (NO_x). This paper experimentally analyses the influence of EGR on smoke and NO_x emissions with ethanol-blended PME.

The results show that the combination of ethanol blending and EGR is effective in reducing NO_x and smoke simultaneously without the thermal efficiency deteriorating. The smoke reduction can be attributed to an improved fuel–air mixing by an increased ignition delay owing to the low cetane number of ethanol and by a promoted fuel spray atomization caused by the low boiling point of ethanol. The increase in the oxygen content also leads to lower soot emission. The decrease in local equivalence ratio by ethanol blending was also suggested by the flame observation in which flame with high luminosity, high temperature, and high KL factor shrinks.

Keywords: biodiesel fuel, FAME, bioethanol, oxygenated fuel, smoke, NO_x, cold flow performance, EGR

1 INTRODUCTION

Biodiesel fuels (BDFs) produced from renewable resources are environmentally friendly alternatives to petroleum diesel fuels. Methyl esters of vegetable oils are easily used in diesel engines without a modification, they cause relatively low soot emissions owing to their oxygen content, and have received increasing attention in many countries [**1**–**2**]. The supply volume of the renewable vegetable oil is a critical factor in the extensive use of BDF as vehicle fuel, when considering the large difference between today's crude oil consumption and vegetable oil production. Among the commercially produced vegetable oils, palm oil has an extremely high productivity as shown in Table 1 [**3**]. Because of this, the palm oil is a very attractive option as the source of BDF, and southeast Asian countries are active in the production and export of palm oil. However, the low-temperature flow properties of palm oil methyl ester (PME) are less favourable than other vegetable-oil-based BDFs, while the cloud points of BDFs are generally higher than petroleum diesel fuels [**4**]. Therefore, to take advantage of the high productivity of palm oil, it is very important to improve the cold flow performance of PME.

Fatty acid methyl esters, such as palmitic acid methyl ester, are the main constituent of BDF. They are highly soluble in ethanol at any level without blending agents, and because ethanol has a very low

**Corresponding author: Division of Energy and Environmental Systems, Hokkaido University, N13 W8, Sapporo, 060-8628, Japan. email: shudo@eng.hokudai.ac.jp*

Table 1 Vegetable oil productivity [**3**]

	Productivity (kg/(m^2 year))
Palm oil	336 (490*)
Rapeseed oil	64
Soybean oil	41–46
Corn oil	42–44

*Including oil from the palm seeds

solidifying temperature, the low-temperature flow properties of BDF can be improved by blending with ethanol [**5**]. In addition, ethanol can also be produced from renewable biomass so that ethanol blending does not spoil the reduction in carbon dioxide emission that the use of BDF brings about. Then, because ethanol has a higher oxygen content, lower cetane number, and lower boiling point than fatty acid methyl esters, ethanol blending into BDF would also have a strong effect on mixture formation, ignition, combustion, and exhaust emissions. The ethanol blending to PME increases the ignition delay and the fraction of premixed combustion, resulting in a dramatic reduction in smoke emission [**5**].

The reduced smoke may be expected to expand the exhaust gas recirculation (EGR) limit and lead to simultaneous reductions of smoke and oxides of nitrogen (NO_x) by combining ethanol blending and EGR in BDF combustion. This paper experimentally analyses the influence of EGR on smoke and NO_x emissions from combustion of ethanol-blended PME in a single-cylinder diesel engine. The mechanisms in the smoke reduction by ethanol blending are also discussed by comparing the effects of additives with different oxygen contents, cetane numbers, and boiling points, and by analysing combustion flame image analyses using the two-colour method.

2 EXPERIMENTS

2.1 Experiments for combustion and exhaust emissions characteristics

The engine used in the experiments for analysing the characteristics of combustion and exhaust emissions was a four-stroke cycle single-cylinder open-chamber type diesel engine with a bore of 92 mm, a stroke of 96 mm, and a compression ratio of 17.7. It was installed with a common rail type fuel injection system. The fuel injection pressure was set at 60 MPa in all of the experimental conditions. In experiments with EGR, a part of the exhaust gas was introduced to the intake of the engine via a water-cooled heat exchanger. The in-cylinder pressure data were measured with a piezoelectric type pressure sensor (KISTLER 6061B) and recorded with an A–D converter (Interface CBI-320412). The pressure data were averaged over 45 cycles for each experimental condition and the averages were used in the calculation of the apparent rate of heat release, in-cylinder gas mean temperature, and efficiency factors.

The exhaust gas concentrations of NO_x were measured with a chemiluminescence detector (CLD) type NO_x analyser (Horiba C5-3013), that of unburned hydrocarbon with a flame ionization detector (FID) type total hydrocarbon analyser (Horiba FIA-52), and that of carbon monoxide with a non-dispersed infrared (NDIR) type CO analyser (Horiba AIA-23). The soot concentration in the exhaust gas was measured with a Bosch type smoke analyser (ZEXEL DSM-20AN).

Blends of PME and ethanol (C_2H_5OH) at different blending ratios were used as the fuel. Table 2 shows the properties of the tested PME, ethanol, and some ethanol/PME blends. Ethyl tertiary butyl ether (ETBE; $C_2H_5OC_4H_9$, boiling point: 72 °C, cetane number: 2.5), iso-octane (C_8H_{18}, boiling point: 99.3 °C, cetane number: 10), and light cyclic oil (LCO; T_{50} = 278 °C, cetane index: 23) were also used as additives to PME for analysing the mechanism in the smoke reduction by ethanol blending.

2.2 Experiments for flame observation and two-colour method analysis

The experiments for flame observation and two-colour method analysis were performed in a bottom-view type optical access engine having an extended piston with a transparent fused silica crown. The engine has a bore of 135 mm, a stroke of 130 mm, and a compression ratio of 18.8, and is equipped with a common rail type fuel injection system. Blends of PME and ethanol at different blending ratios were used as the fuel. The combustion flame images were recorded by a memory type high-speed video camera (Photoron Fastcam-ultima-RGB). Imaging was made with a constant aperture and frame speed of 9000 fps.

3 RESULTS AND DISCUSSIONS

3.1 Cold flow performance of BDF/ethanol blends

Despite the important advantage of productivity of palm oil, PME has poorer cold flow performances than other vegetable-oil-based biodiesel fuels. The cloud point of PME is around 14 °C, and it is difficult

Table 2 Properties of the tested PME, ethanol, and ethanol-blended PME

	PME	Ethanol[f]	E20PME	E40PME
Methyl palmitate (16:0)	44.6 wt%	—	36.7 wt%	27.7 wt%
Methyl stearate (18:0)	5.8 wt%	—	4.8 wt%	3.6 wt%
Methyl oleate (18:1)	39.5 wt%	—	32.5 wt%	24.6 wt%
Methyl linoleate (18:2)	8.8 wt%	—	7.2 wt%	5.5 wt%
Ethanol (C_2H_5OH)	—	99.9 wt%	17.7 wt%	37.8 wt%
Cetane number	65.8[a]	8	(54.2[g])	(42.7[g])
Oxygen content	13.2 wt%[b]	34.8 wt%	26.2 wt%	21.8 wt%
Boiling point	215 ~ 443 °C[c]	78.3 °C	78.3 ~ 443 °C	78.3 ~ 443 °C
Solidifying point	—	−114 °C	—	—
Flash point	—	13 °C	—	—
Density	0.855 g/cm^3 [d]	0.794 g/cm^3	(0.843 g/cm^3 [h])	(0.831 g/cm^3 [h])
Lower heating value	37.26 MJ/kg[e]	26.82 MJ/kg	35.17 MJ/kg	33.08 MJ/kg

[a]measured in CFR engine, [b]measured in CHON elemental analyser, [c]estimated from reference [**6**], [d]measured at 40 °C, [e]calculated from measured higher heating value and measured hydrogen content, [f]data for ethanol from reference [**7**], [g]calculated from volumetric mixing ratio and each cetane number, [h]calculated from volumetric mixing ratio and each density.

to utilize neat PME as vehicle fuel except for in tropical countries. To exploit the high productivity of palm oil and use PME in a wide range of regions including colder countries, it is crucial to improve the cold flow performances of PME. PME contains a large amount of the palmitic acid methyl ester ($CH_3(CH_2)_{14}COOCH_3$) having a solidifying temperature of 30.5 °C. The high fraction of saturated fatty compound is one reason for the high cloud point of PME. Methyl esters of vegetable oils, BDF, are mixtures of several kinds of fatty ester, and they are highly soluble in ethanol at any level without blending agents. Because the solidifying temperature of ethanol is a low −114 °C, ethanol blending into BDF is expected to lower the cloud point [**5**]. Figure 1 shows measured cloud points of PME/ethanol blends for different ethanol fractions, showing that ethanol blending effectively lowers the cloud point. At 40 vol% of ethanol blending the cloud point is approximately 8 °C, about 6° lower than the cloud point of neat PME. The ethanol blending expands the region where PME can be used for vehicles. The effect by ethanol blending to lower the cloud point was also confirmed with rapeseed oil methyl ester (RME).

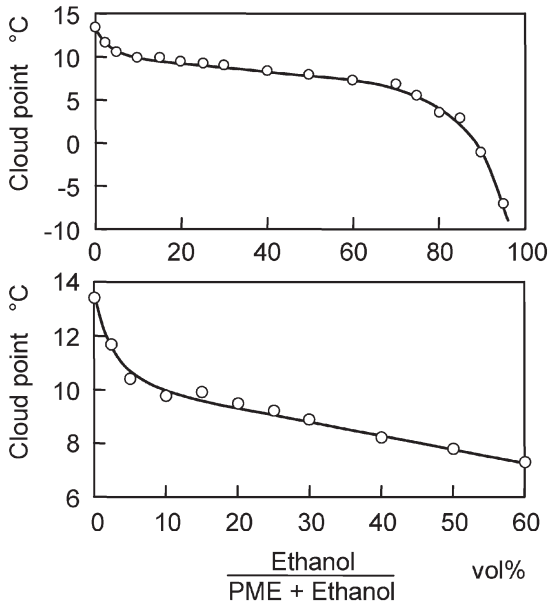

Fig. 1 Cloud point with ethanol-blended PME

3.2 Influences of ethanol blending to BDF on combustion and exhaust emissions

Compared with PME, ethanol has a lower cetane number, lower boiling point, and higher oxygen content as shown in Table 2. Because of this, the ethanol blending into PME would have influences on mixture formation, ignition, combustion, and exhaust emissions. Figure 2 shows the experimental results of the combustion of the ethanol-blended PME. The ethanol fraction in the blend fuel was set at 0, 20, and 40 vol%. The fuel injection timing was set at 8° crank angle (CA) before top dead centre (BTDC). Smoke, which tends to increase with engine load, decreases with increasing in the ethanol content. The ethanol blending hardly influences the NO_x emission and the brake thermal efficiency η_e in the conditions set here. The influence of the ethanol blending on total hydrocarbon (THC) and CO emissions is limited. Therefore, the ethanol blending can reduce the smoke emission considerably without a remarkable deterioration in other exhaust emissions and thermal efficiency.

Figure 3 shows measured in-cylinder pressure P, apparent rate of heat release $dQ/d\theta$, and the in-cylinder gas mean temperature T_g with the PME/ethanol blended fuels with the different ethanol contents [**5**]. The fuel injection timing was set at 5° CA BTDC, the brake mean effective pressure

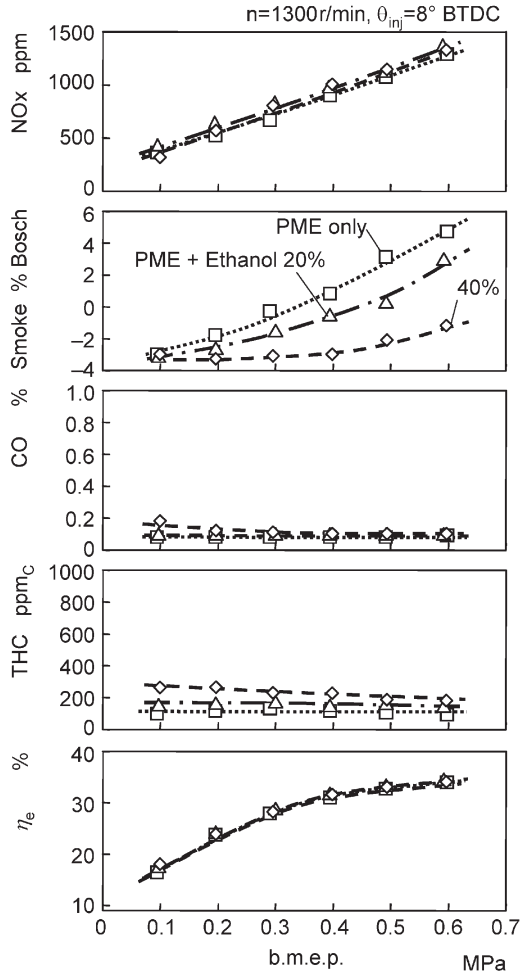

Fig. 2 Influence of ethanol blending on exhaust emissions and thermal efficiency in PME combustion

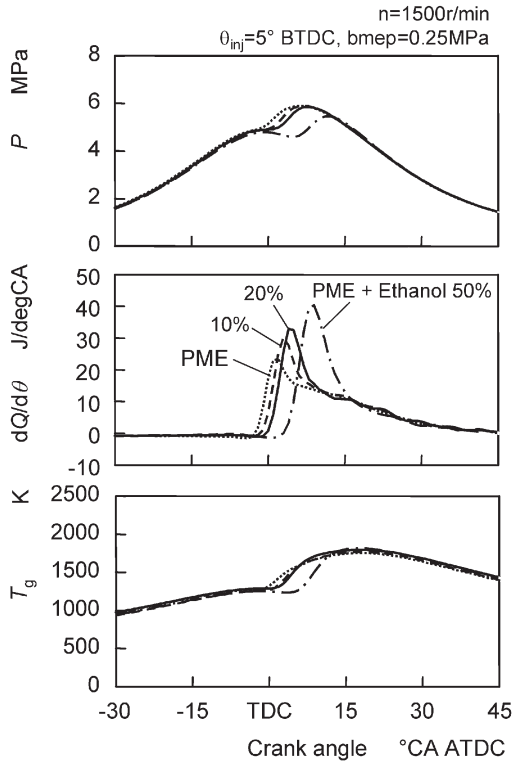

Fig. 3 Influence of ethanol blending on in-cylinder pressure, apparent rate of heat release, and in-cylinder gas mean temperature in PME combustion [**5**]. ATDC: after top dead centre

(b.m.e.p.) was 0.25 MPa, and the apparent rate of heat release $dQ/d\theta$ was calculated from the measured pressure data P by the following equation [**8**, **9**]

$$dQ/d\theta = (V dP/d\theta + \gamma P dV/d\theta)/(\gamma - 1) - PV/(\gamma - 1)^2 d\gamma/d\theta \quad (1)$$

Here, V and γ are volume and specific heat ratio of the in-cylinder gas, and θ is the crank angle.

The results in Fig. 3 show that the ignition timing is retarded as the content of ethanol is increased. The cetane number of ethanol is 8, while that for the tested PME was 65.8. The retarded ignition timing increases the apparent rate of heat release during the first-stage combustion that is mostly premixed combustion. This suggests that the ethanol blending increases the amount of fuel–air mixture that is formed during the ignition delay. Improvement in the evaporation of injected fuel by blending ethanol may also be a reason for the increased premixed combustion, because the ethanol has a far lower boiling point compared with the tested PME. The boiling point of ethanol is 78.3 °C, while fatty acid methyl esters in PME have boiling points from 215 to 443 °C, as shown in Table 2. The smoke reduction indicated by Fig. 2 may be attributed to the increased fraction of premixed combustion and also to an increase in the oxygen content of the blended fuels. On the other hand, the maximum value of the in-cylinder gas mean temperature is hardly influenced by the ethanol blending in spite of the large increase in the premixed combustion heat release as shown in Fig. 3. This is because of the largely retarded combustion phase with the ethanol blending and can be a reason for the small change in NO_x emissions shown in Fig. 2.

While the ethanol blending strongly affects the ignition timing as shown in Fig. 3, thermal efficiency changes little with the blending as shown in Fig. 2. To better understand this, thermal efficiency factors in the combustion of PME/ethanol blends were analysed by using the measured pressure data.

The brake thermal efficiency of an engine η_e can be expressed with the theoretical thermal efficiency

of the Otto cycle η_{th}, the degree of constant volume η_{glh}, the combustion efficiency η_u, the cooling loss fraction ϕ_w, and the mechanical efficiency η_m [**10**]

$$\eta_e = \eta_m \eta_{th} \eta_{glh} \eta_u (1 - \phi_w) \tag{2}$$

This equation can be rewritten with diagram factor η_g [**8**, **11**]

$$\eta_e = \eta_m \eta_{th} \eta_g \tag{3}$$

The diagram factor η_g is expressed with the degree of constant volume η_{glh}, the combustion efficiency η_u, the cooling loss fraction ϕ_w, and the factor governs the trends of brake thermal efficiency η_e in an engine at a load. The degree of constant volume η_{glh} is expressed by equation (4) [**8**, **11**]. The degree of constant volume indicates how close the apparent heat release is to the constant volume heat input at the top dead centre, which is assumed in the Otto cycle

$$\eta_{glh} = 1/(\eta_{th} Q) \int \left\{ 1 - \left[(V_h + V_c)/V^{1-\gamma} \right] \right\} \mathrm{d}Q/\mathrm{d}\theta \mathrm{d}\theta \tag{4}$$

Here, Q is the cumulative apparent heat release, V_h is the stroke volume, and V_c is the clearance volume. The value of $\eta_u(1 - \phi_w)$, comprising the combustion efficiency η_u and the cooling loss fraction ϕ_w, was obtained from the cumulative apparent heat release Q and supplied fuel energy Q_{fuel} per cycle [**8**]. The cumulative apparent heat release Q, which is influenced by the heat transfer from burning gas to combustion chamber wall, can be described with cumulative real heat release Q_B and the cumulative cooling loss Q_C in a cycle

$$Q/Q_{fuel} = (Q_B - Q_C)/Q_{fuel} \tag{5}$$

The cumulative cooling loss Q_C is total heat transferred from burning gas to the cylinder walls in a cycle. The cumulative real heat release Q_B corresponds to the product of the supplied fuel energy Q_{fuel} and the combustion efficiency η_u

$$Q/Q_{fuel} = \eta_u (Q_B - Q_C)/Q_B \tag{6}$$

The cooling loss fraction ϕ_w was defined as a fraction of the cumulative cooling loss heat Q_C to the cumulative real heat release Q_B

$$Q/Q_{fuel} = \eta_u (1 - \phi_w) \tag{7}$$

Figure 4 shows the thermal efficiency factors for the experimental results in Fig. 3. A large amount of

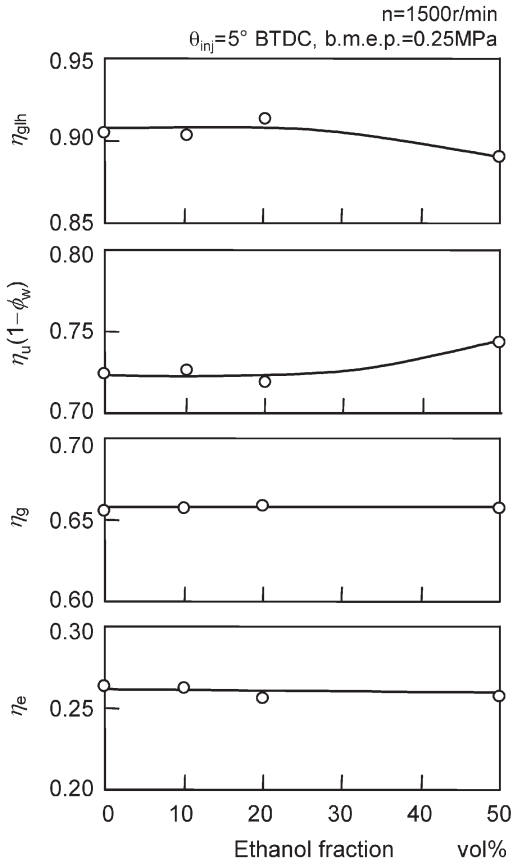

Fig. 4 Influence of ethanol addition on thermal efficiency factors [**5**]

ethanol blending tends to decrease the degree of constant volume η_{glh} owing to the retarded ignition timing, but the increase in the value of $\eta_u(1 - \phi_w)$ maintains the diagram factor η_g and the brake thermal efficiency η_e. Because changes in the theoretical thermal efficiency η_{th} and the mechanical efficiency η_m are small, the brake thermal efficiency η_e is influenced mostly by the changes in the diagram factor η_g, which consists of the degree of constant volume η_{glh} and $\eta_u(1 - \phi_w)$. Most of the increase in $\eta_u(1 - \phi_w)$ can be attributed to a decrease in the cooling loss fraction ϕ_w owing to a shortened contact time for burning gas and combustion chamber walls due to the retarded combustion phase. The possible change in flame luminosity by increased premixed combustion fraction with ethanol blending may also lead to a decreased radiation heat transfer.

3.3 Influences of ethanol blending to BDF and EGR on combustion and exhaust emissions

The reduced smoke resulting from the ethanol blending could allow an expansion of the EGR limit, and a combination of ethanol blending and EGR

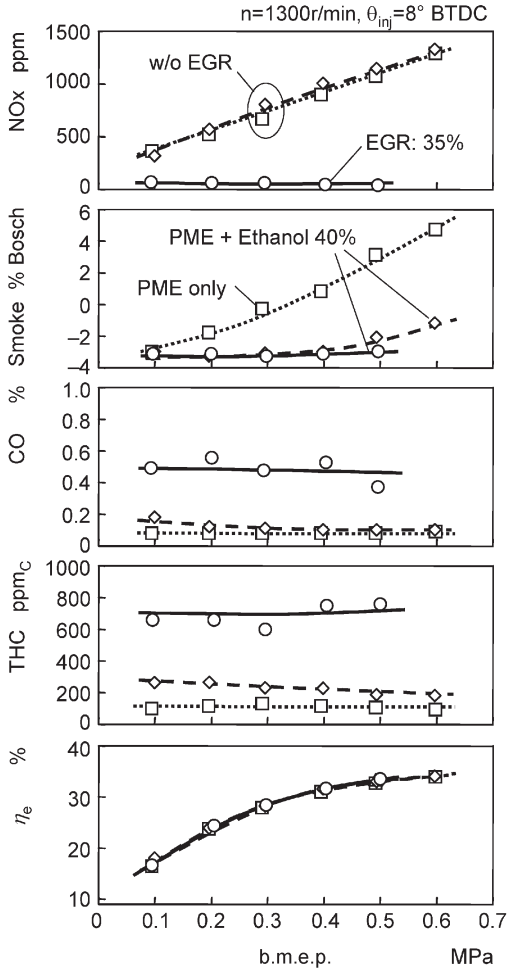

Fig. 5 Influence of ethanol blending and EGR on exhaust emissions and thermal efficiency in PME combustion

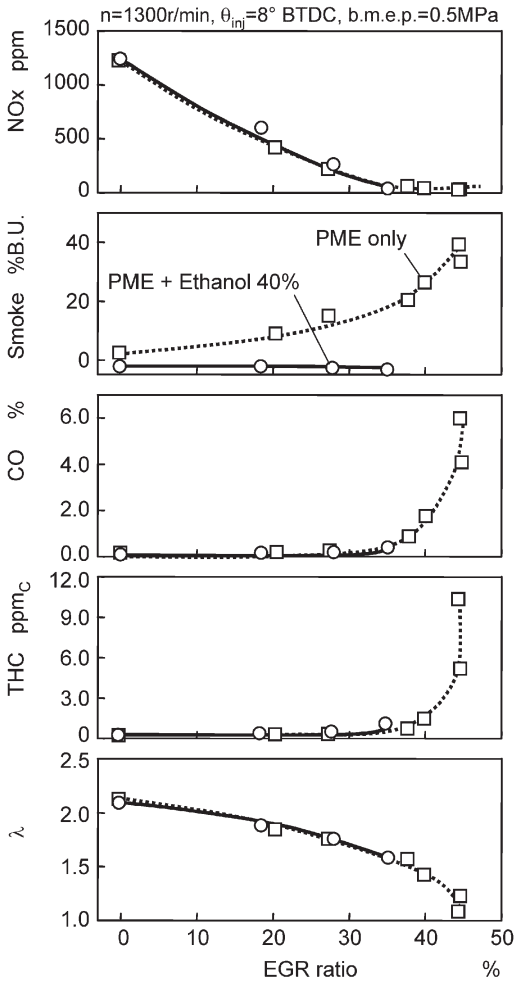

Fig. 6 Influence of EGR on exhaust emissions and thermal efficiency in ethanol-blended PME combustion

could simultaneously reduce soot and NO_x in PME combustion. Figure 5 shows the experimental results with combustion of the 40 vol% ethanol blended PME with 35 per cent EGR: 35 per cent was the maximum EGR ratio without deteriorating thermal efficiency. The results with neat PME and 40 vol% ethanol-blended PME without EGR are also shown in the figure for comparison. The fuel injection timing was set at 8° BTDC. With EGR, NO_x emissions are considerably reduced, maintaining the large smoke reduction effect by ethanol blending. Although THC and CO emissions are slightly increased, the brake thermal efficiency is hardly influenced by EGR. The emissions of THC and CO are not very high and could be after-treated by oxidation catalysts.

Figure 6 shows the influence of EGR ratio on exhaust emissions and thermal efficiency in the combustion of 40 vol% ethanol blended PME. Results with neat PME are also shown in the figure for a comparison. The fuel injection timing was set at 8° CA BTDC, and the b.m.e.p. was at 0.5 MPa. The excess air ratio, which decreases with an increase in the EGR ratio, is around 2.1 for without EGR and around 1.6 for 35 per cent EGR. While NO_x is decreased with an increase in EGR ratio, smoke from neat PME combustion is remarkably increased. However, the ethanol-blended PME maintains the relatively low smoke level, and the combination of ethanol blending and EGR can achieve the simultaneous reduction of NO_x and smoke. THC and CO emissions are hardly influenced by EGR below the 35 per cent EGR ratio. Although the 40 vol% ethanol blended PME sometimes causes misfiring with EGR by more than 35 per cent at the fixed fuel injection timing of 8° CA BTDC, an injection timing advance enables the blend fuel to operate at EGR ratios higher than 35 per cent. Figure 7 shows the relation between NO_x and smoke emissions at a fuel injection timing of 8° BTDC and b.m.e.p. of

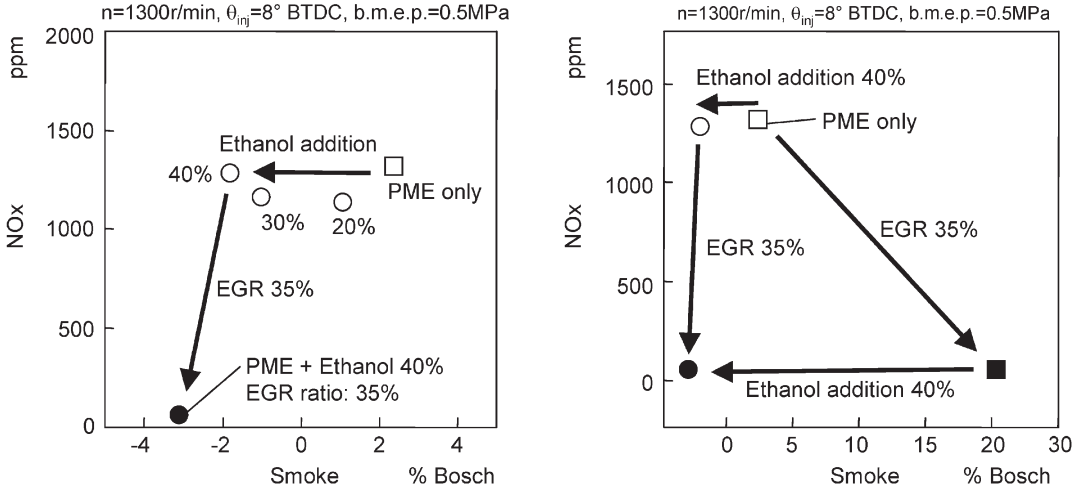

Fig. 7 Influence of ethanol blending and EGR on the NO_x and smoke relation

0.5 MPa. Ethanol blending and EGR substantially ease the trade-off between NO_x and smoke.

Therefore, the combination of ethanol blending and EGR can be a very effective technique to achieve simultaneous reductions in NO_x and smoke emissions without deteriorating thermal efficiency in BDF combustion.

3.4 Flame observation and two-colour method analysis with ethanol blended BDF

Previous sections signify that the ethanol blending to PME decreases the fraction of diffusion combustion, which tends to emit a larger amount of soot than premixed combustion. To confirm this, a combustion flame was observed with a bottom-view type optical access engine and was analysed by the two-colour method. The engine was operated at the b.m.e.p. of 0.5 MPa, the fuel injection timing of 5° CA BTDC, the engine speed of 900 r/min, and the fuel injection pressure of 120 MPa. Imaging was made by a high-speed colour video camera with a constant aperture and frame speed of 9000 fps.

Figure 8 shows direct flame images of PME combustion with ethanol blending by 0, 10, and 20 vol %. Figure 9 shows the averaged luminosity of the flame images against crank angle. The images indicate that ethanol blending decreases the averaged flame luminosity and the region of luminous flame, which were probably caused by the decrease in the fraction of diffusion combustion flame which has far higher emissivity than the premixed combustion flame. The 20 vol % ethanol blending reduces the maximum average flame luminosity to less than half that with

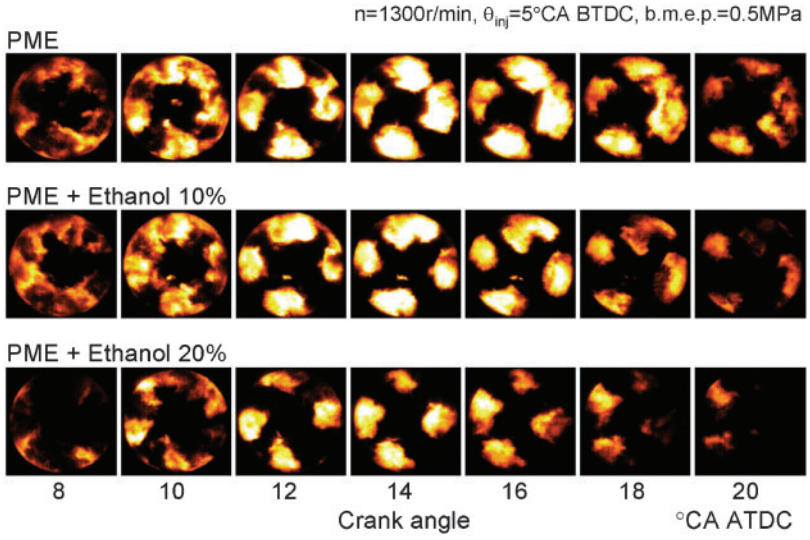

Fig. 8 Flame images of ethanol-blended PME combustion

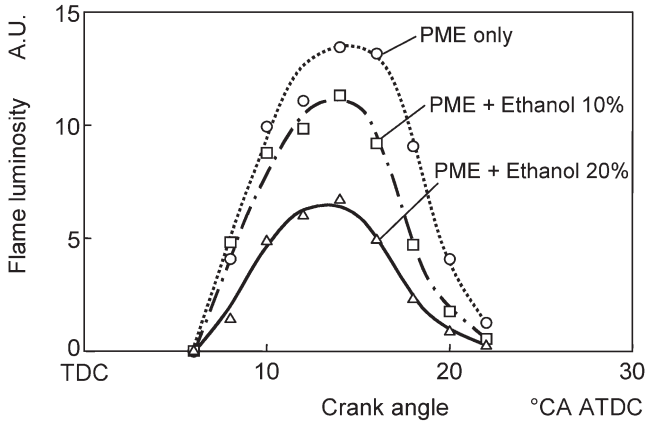

Fig. 9 Influence of ethanol blending on average flame luminosity

neat PME. The decrease in the cetane number by the ethanol blending can be a main reason for the decreased diffusion combustion fraction, because the retarded ignition timing increases the time available for fuel–air mixing before ignition. The improved evaporation of injected fuel by blending ethanol with a low boiling point can also be a reason for the decreased diffusion combustion fraction. The retarded ignition timing and the increased premixed combustion fraction by the ethanol blending are also clearly indicated in Fig. 3. The less luminous flames with ethanol blending also lead to the decreased radiation heat transfer from burning gas to the cylinder walls and can be a reason for the low cooling loss fraction shown in Fig. 4.

The luminous flame emission in diesel combustion is thermal radiation from soot particles formed in flame, and the monochromatic radiation heat flux E_λ at a wavelength λ is a function of the flame temperature T and the monochromatic emissivity of soot particles group ε_λ [**12**].

$$E_\lambda = \varepsilon_\lambda C_1 / \{\lambda^5 [\exp(C_2/\lambda T) - 1]\} \tag{8}$$

Here, C_1 and C_2 are constants. The monochromatic emissivity ε_λ in the equation can be expressed with the following equation [**13**, **14**].

$$\varepsilon_\lambda = 1 - \exp(KL/\lambda^\alpha) \tag{9}$$

The KL factor, with the absorption coefficient of soot particles K and flame thickness L, corresponds to a relative index for soot concentration. Measurements at two wavelengths give the flame temperature T and the relative soot concentration KL by choosing a proper value for α in equation (9) [**11**]. This two-colour method is consistent for measuring the flame temperature of the diesel engine by using 1.38 for the exponent on wavelength α [**14**]. Figures 10 and 11 show distributions of flame temperature and KL factor derived with the two-colour method from the flame images shown in Fig. 8. The calculation was carried out on each pixel of the recorded flame images, employing 1.38 for the value of α. With increases in the ethanol fraction, flames with high temperature and high KL factor shrink. This suggests that the increased ignition delay and improved fuel

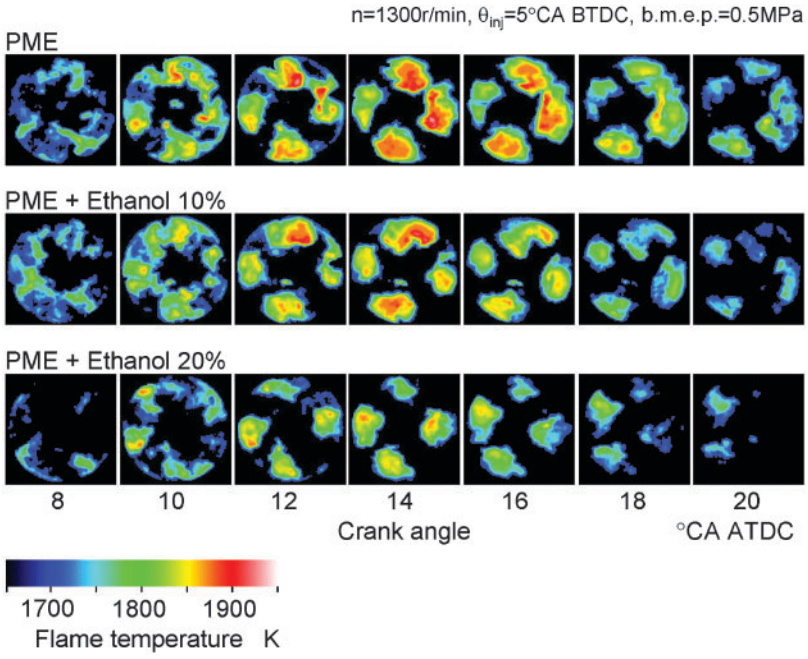

Fig. 10 Flame temperature distribution in ethanol-blended PME combustion

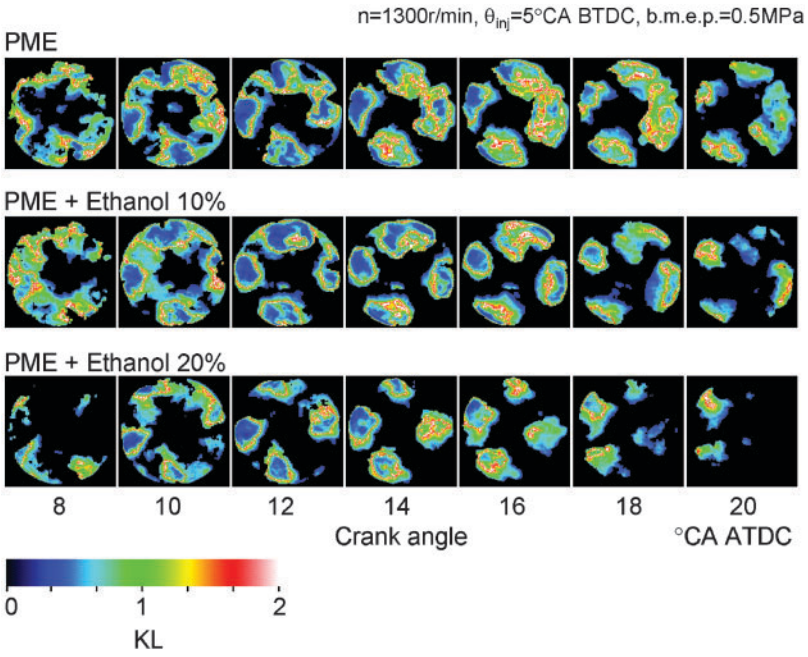

Fig. 11 Distribution of KL factor in ethanol-blended PME combustion flame

evaporation by ethanol blending promoted fuel–air mixing and reduced the region with high local equivalence ratio. The decrease in the region with high local equivalence ratio suppresses the soot formation. The increase in fuel oxygen content by blending ethanol may also have an effect on the shrinkage of high *KL* flame region.

3.5 Mechanism in smoke reduction by ethanol blending to BDF

This section analyses the mechanism of smoke reduction by ethanol blending in PME combustion. The analysis focuses on the influence of the changes in cetane number, oxygen content, and volatility of the fuel on the smoke emissions.

Figure 12 shows results with blends of PME and ethanol (oxygen content: 34.8 wt%, cetane number: 8), ETBE (oxygen content: 15.7 wt%, cetane number: 2.5), or iso-octane (oxygen content: 0 wt%, cetane number: 10). The fuel injection timing was set at 8° BTDC, and the b.m.e.p. was 0.5 MPa for all the cases. The EGR ratio was set at 35 per cent. The figure shows oxygen content, cetane number, and smoke against the fraction of the additive fuels. The cetane numbers plotted in the figure were estimated with the volumetric mixing ratio of PME and the additives. The differences in estimated cetane number among the three kinds of blended fuel are quite small at the blending ratios tested here. All cases show decreases in cetane number and reductions in smoke, and this

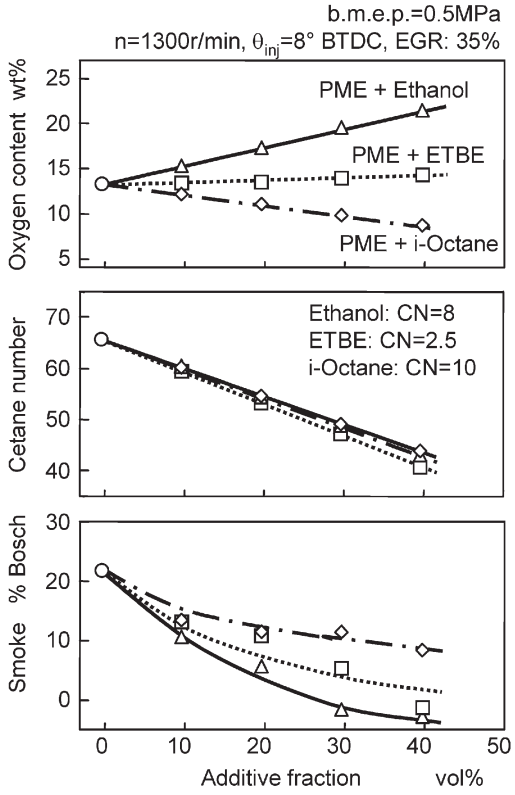

Fig. 12 Influence of oxygen content and cetane number of additive fuels on smoke reduction

indicates that the main reason for the smoke reduction is increased ignition delay by the decreased cetane number. Among the three cases, the additive with higher oxygen content gives the larger effect of

smoke reduction. It suggests that the increase in oxygen content may be a factor for the smoke reduction by ethanol blending into PME.

Because most fatty acid methyl esters contained in PME have boiling points from 215 to 443 °C, blending ethanol with a boiling point of 78.3 °C changes volatility characteristics considerably. In addition to the decrease in cetane number, improved volatility may also increase the premixed combustion fraction. To separate this effect, two kinds of additive with very different volatilities and with similar cetane number and oxygen content were investigated. Figure 13 shows the results for PME blended with iso-octane (C_8H_{18}, boiling point: 99.3 °C) and light cyclic oil (LCO; $T_{50} = 278$ °C) by 20 vol%. Volatility characteristics of the tested additives for the blending are shown in Fig. 14. Palmitic acid methyl ester, the main constituent of PME, has a very high boiling point of 418 °C. The graph in Fig. 13 shows oxygen content, ignition delay, premixed combustion fraction, and smoke emission for the two blend fuels. The premixed combustion fraction was obtained by analysing the heat release. The apparent rate of heat release $dQ/d\theta$ was integrated from ignition to the crank angle with the maximum rate of heat release as shown in Fig. 15. Then the value was doubled to obtain the approximate value of cumulative heat release by the first stage combustion Q_{pre} which is mostly premixed combustion. The premixed combustion fraction was defined as a fraction of the premixed combustion heat release Q_{pre} to the total apparent heat release Q.

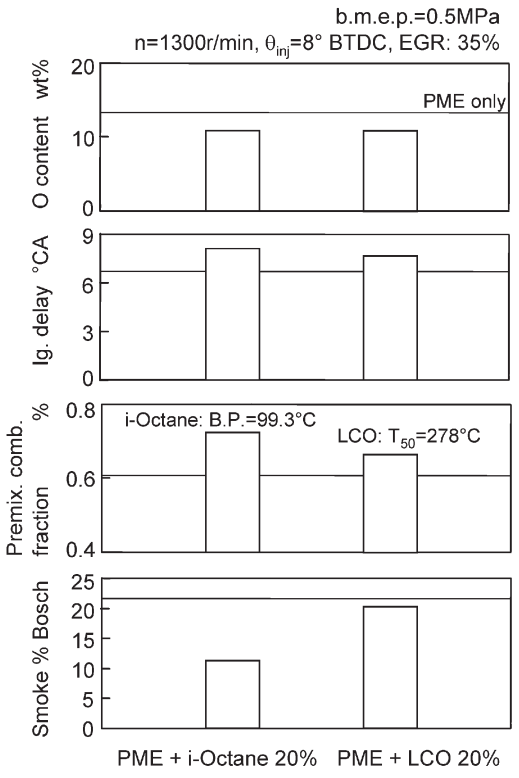

Fig. 13 Influence of volatility of additive fuels on smoke reduction

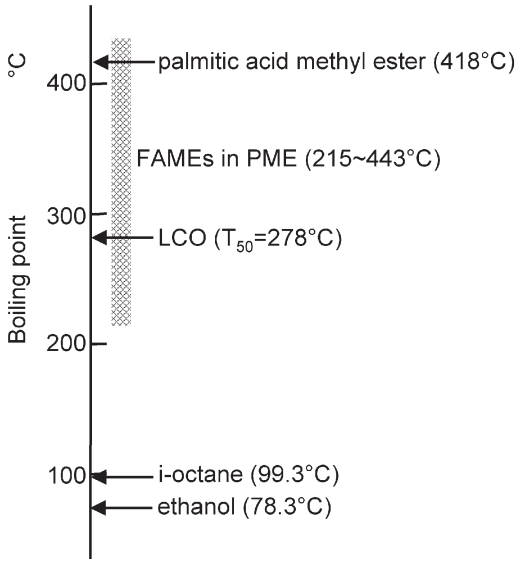

Fig. 14 Volatility of the tested fuels

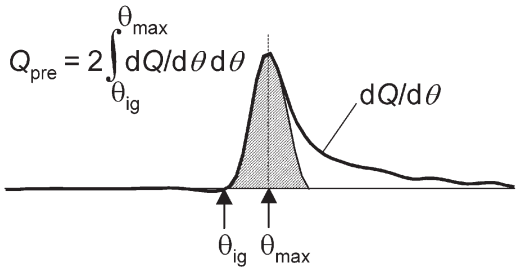

Fig. 15 Estimation of premixed combustion heat release

Neither iso-octane nor LCO contains oxygen, but both have quite low cetane numbers. The difference in estimated cetane numbers with the two kinds of blended fuel is quite small at the 20 vol% blending ratio here, resulting in similar ignition delays. With iso-octane there is a larger fraction of premixed combustion and a stronger effect of smoke reduction. Here, molecular structure of some compounds in LCO, which contains aromatic hydrocarbons, is largely different from that of iso-octane. Therefore the smoke emission tendencies of the two additives themselves are different from each other. However, the contributions of the additives to the smoke emission from the blended fuels would be small at the 20 vol% blending ratio, considering that the volatility of the additives is significantly better than the main constituent of PME having 418 °C boiling point. The improved fuel volatility by blending

ethanol with the much lower boiling point than PME may also be a factor in the increased premixed combustion and smoke reduction.

Therefore, the main factors in the smoke reduction by ethanol blending into PME are the increased premixed combustion due to the decreased cetane number and the improved volatility, and the increased oxygen content. These effects can also be achieved with other diesel fuels by blending a fuel having a low cetane number, a low boiling point, and high oxygen content.

4 CONCLUSION

The results of this study may be summarized as follows.

1. Despite the important advantage of the productivity of palm oil, PME has poorer cold flow performances than other vegetable-oil-based biodiesel fuels. Fatty acid methyl esters, the main constituents of PME, are highly soluble in ethanol at any level without blending agents, and cloud point can be lowered by blending ethanol to PME. While the cloud point of neat PME is around 14 °C, 40 vol % ethanol blending brings 8 °C cloud point.
2. Smoke emissions from diesel combustion of ethanol-blended PME decrease with increasing ethanol fraction. The first stage heat release, which is mostly by premixed combustion, is increased with the ethanol blending and the smoke reduction. By blending ethanol to PME, flame region with high luminosity, high temperature, and high *KL* factor shrink. This suggests that the ethanol blending increases premixed combustion and reduces the region with high local equivalence ratio, which leads to the soot formation.
3. The smoke reduction effect by the ethanol blending to PME is maintained in the operation with EGR resulting in reduced NO_x. The thermal efficiency is hardly influenced by 40 vol % ethanol blending and 35 per cent EGR. The combination of ethanol blending and EGR would be effective in reducing NO_x and smoke simultaneously without deteriorating the thermal efficiency in PME combustion. The trade-off between NO_x and smoke can be considerably eased by this technique.
4. The smoke reduction by blending ethanol can be attributed to an improved fuel–air mixing, which results in increased premixed combustion and decreased diffusion combustion, by an increased ignition delay owing to the low cetane number of ethanol and by a promoted evaporation of fuel spray resulting from the relatively low boiling point of ethanol. The increase in the oxygen content in the blended fuel also leads to the lower soot emission. These effects can also be achieved with other diesel fuels by blending a fuel having a lower cetane number, lower boiling point, and higher oxygen content.

ACKNOWLEDGEMENTS

The author expresses gratitude to Mr Atsushi Fujibe, Mr Motoharu Kazahaya, and Mr Shuji Yamamoto, (former students of Kitami Institute of Technology), Mr Takuya Yoshida, Mr Hirotaka Takeuchi, Mr Yukihiro Ishida, Mr Keisuke Sasaki, and Mr Hari Setiapraja (students of Hokkaido University), for help in the experiments.

REFERENCES

1 **Choi, C. Y., Bower, G. R.,** and **Reitz, R. D.** Effects of biodiesel blended fuels and multiple injections on D.I. diesel engines. SAE paper 970218, 1997.
2 **Yamane, K., Ueta, A.,** and **Shimamoto, Y.** Influence of physical and chemical properties of biodiesel fuel on injection, combustion and exhaust emission characteristics in a direct injection compression ignition engine. *Int. J. Engine Res.*, 2001, **2**(JER4), 249–261.
3 **Yamada, J.** and **Tanaka, Y.** Manufacturing process of bio-diesel fuel. *Engine Technol.*, 2003, **5**(5), 45–51. In Japanese.
4 **Huan, C.** and **Wilson, D.** Improving the cold flow properties of biodiesel. In Proceedings of the 91st AOCS Annual Meeting, San Diego, 2000.
5 **Shudo, T., Fujibe, A., Kazahaya, M., Aoyagi, Y., Ishii, H., Goto, Y.,** and **Noda, A.** The cold flow performance and the combustion characteristics with ethanol blended biodiesel fuel. SAE paper No. 2005-01-3707, 2005.
6 **Knothe, G.** Dependence of biodiesel fuel properties on the structure of fatty acid alkyl esters. *Fuel Processing Technol.*, 2005, **86**, 1059–1070.
7 **Saka, S.** Perspectives of biomass energy and its substitute for fossil fuels. *Engine Technol.*, 2001, **3**(3), 29–34. In Japanese.
8 **Shudo, T., Nabetani, S.,** and **Nakajima, Y.** Analysis of the degree of constant volume and cooling loss in a spark ignition engine fuelled with hydrogen. *Int. J. Engine Res.*, 2001, **2**(JER1), 81–92.
9 **Shudo, T., Nabetani, S.,** and **Nakajima, Y.** Influence of specific heats on indicator diagram analysis

in a hydrogen-fuelled SI engine. *JSAE Rev.*, 2001, **22**(2), 224–226.

10 **List, H.** *Thermodynamik der Verbrennungskraftmaschinen*, 1939 (Springer-Verlag, New York).

11 **Shudo, T.** Improving thermal efficiency by reducing cooling losses in hydrogen combustion engines. *Int. J. Hydrogen Energy*, 2007, **32**(17), 4285–4293.

12 **Plank, M.** *The theory of heat radiation*, 1959 (Dover Publication, New York).

13 **Hottel, H. C.** and **Broughton, F. P.** Determination of true temperature and total radiation from luminous gas flames: use of special two-color optical pyrometer. *Ind. Engng Chemistry*, 1932, **4**(2), 166–175.

14 **Matsui, Y., Kamimoto, T.,** and **Matsuoka, S.** A study on the time and space resolved measurement of flame temperature and soot concentration in a DI diesel engine by the two-color method. SAE paper No. 790491, 1979.